Letter

Suppression of shot noise in a dirty marginal Fermi liquid

Tsz Chun Wu[1] and Matthew S. Foster[1,2]
[1]Department of Physics and Astronomy, Rice University, Houston, Texas 77005, USA
[2]Rice Center for Quantum Materials, Rice University, Houston, Texas 77005, USA

(Received 20 December 2023; revised 30 April 2024; accepted 16 July 2024; published 1 August 2024)

We study shot noise in a two-dimensional, disordered marginal Fermi liquid (MFL) driven out of equilibrium. We consider electrons with Planckian dissipation on the Fermi surface coupled to quantum-critical bosons in the presence of disorder. In the noninteracting and strong electron-boson drag limits, MFL effects disappear and our theory reproduces known results. For the case where the bosons remain in equilibrium, inelastic scattering strongly suppresses the noise by dissipating the injected energy. Interestingly, we find that MFL effects do play a role in this regime, and give a weak *enhancement* on top of the otherwise strong suppression. Our results suggest that shot noise can be strongly suppressed in quantum-critical systems, and this scenario may be relevant to recent measurements in a heavy-fermion strange metal.

DOI: 10.1103/PhysRevB.110.L081102

Introduction. Shot noise in electronic transport measures the correlation of current fluctuations

$$S_{\text{shot}} = \int dt \langle \delta\hat{I}(t)\delta\hat{I}(0) + \delta\hat{I}(0)\delta\hat{I}(t)\rangle, \tag{1}$$

when the system is driven out of equilibrium by a voltage V [1,2], where $\delta\hat{I}(t) = \hat{I}(t) - \langle I\rangle$ is the current fluctuation and t is time. The associated Fano factor $\mathsf{F} = S_{\text{shot}}/(2\,e\,I)$ (e is the electric charge, and $I = \langle I\rangle$ is the electric current) offers a unique way to probe the effective charge of carriers in mesoscopic systems, such as superconductor tunneling junctions [3], fractional quantum Hall devices [4,5], and quantum-dot Kondo systems [6,7].

Shot noise in a diffusive wire has been widely studied [1,2,8–16]. In the noninteracting limit, $\mathsf{F} = 1/3$ due to the Dorokhov statistics [1,10,11,14,15]. In the presence of electron-electron interactions, F acquires a nonuniversal enhancement at weak coupling [14] and becomes universal $\mathsf{F} = \sqrt{3}/4$ at $T = 0$ (T is temperature) in the strongly interacting hydrodynamic limit [13,14]. Meanwhile, inelastic electron-phonon scattering suppresses F in a nonuniversal manner [10,16].

In a recent experiment, shot noise measurements on a heavy-fermion strange metal $YbRh_2Si_2$ reveal a strongly suppressed Fano factor F [17]. Experimental determination of the electron-phonon coupling seemingly rules out electron-phonon scattering as the mechanism [10,16]. This intriguing result calls for a new theoretical description of shot noise in quantum-critical systems without well-defined quasiparticles.

In this Letter, we investigate the shot noise in a two-dimensional (2D), disordered marginal Fermi liquid (MFL) [18,19]. In this model, electrons are strongly coupled to quantum-relaxational bosons in the presence of quenched disorder, leading to electronic Planckian dissipation. Our main physical result is that the *adjusted* Fano factor

$$\mathsf{F}_{\text{adj}}(T,V) \equiv (S_{\text{shot}} - S_{\text{JN}})/(2\sigma_D eV), \tag{2}$$

which characterizes the excess noise, is strongly suppressed when the quantum-critical bosons remain in equilibrium. Here, $S_{\text{JN}} = 4T\sigma_D$ denotes the equilibrium Johnson-Nyquist noise and σ_D is the Drude conductivity. Throughout this Letter, we adopt the units $k_B = \hbar = 1$.

A regime wherein bosons remain in equilibrium can arise when interactions among critical fluctuations dominate the boson kinetics, instead of boson-fermion scattering. The corresponding F_{adj} as a function of eV/T is illustrated in Figs. 1(a) and 1(b) for different values of the dimensionless squared boson-fermion coupling $\bar{g}^2 = g^2/(4\pi^2\gamma_{\text{el}})$. Here, γ_{el} is the impurity scattering rate. Excess noise is determined by the critical interaction through the electron temperature T_{e} [Eq. (3), below] and the MFL correction to the shot noise. The former is suppressed by the rate of inelastic electron-boson scattering [10,16], while the latter slightly enhances the Fano factor due to nonequilibrium effects. We quantify the MFL correction through the ratio $\mathcal{R}$ illustrated in Figs. 1(c) and 1(d). The parameter $a \equiv \alpha/\alpha_m$ labeling these plots is inversely proportional to the thermal mass m_{b}^2 of the bosons [see Eq. (6)]. Overall, a lighter thermal mass (larger a) screens the quantum-critical interaction less and thus boosts the suppression. Notably, we find that F_{adj} can fall well below 1/3.

In the crossover regime where $eV \gtrsim T$, F_{adj} decreases as T increases [Figs. 1(a) and 1(b)], in agreement with the recent experimental observation [17]. We find an effective electron temperature that is spatially homogeneous except near the contacts (see Fig. 4), given by

$$T_{\text{e}} \simeq [\theta_{\bar{g}}\, D(eE)^2 + T^3]^{1/3}, \tag{3}$$

where $\theta_{\bar{g}}^{-1} \equiv 2\pi\zeta(3)\bar{g}^2$, D is the diffusion constant, and E is the applied electric field. As the interaction strength $\bar{g}^2$ increases, energy is transferred more rapidly from the electrons to the bosons, which serve as a heat sink, resulting in a more suppressed T_{e}. Equation (3) holds for $a \gtrsim 1$. For $a \ll 1$, a weaker (roughly 1/4) power-law is instead obtained,

$$T_{\text{e}}(a \ll 1) \sim [(c/a\bar{g}^2)T\, D(eE)^2 + T^4]^{1/4}, \tag{4}$$

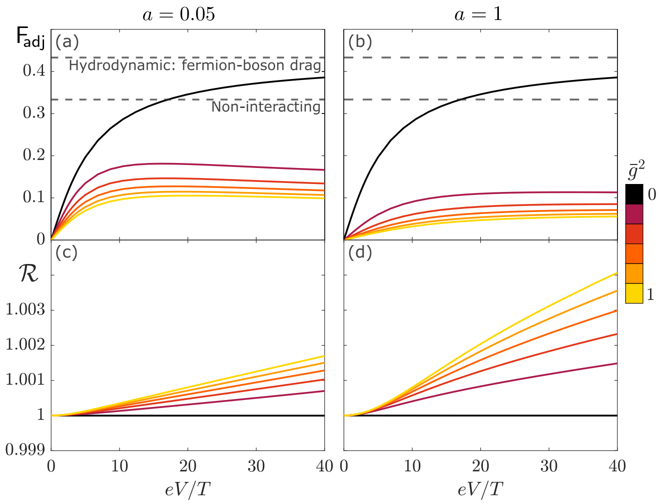

FIG. 1. (a), (b) Plot of the adjusted Fano factor F_{adj} [Eq. (2)] and (c), (d) the marginal-Fermi-liquid (MFL) correction factor $\mathcal{R}$ [Eq. (25)]. The latter arises due to the combination of Planckian dissipation (the MFL self-energy) and the Maki-Thompson diagram shown in Fig. 3(b). All results are plotted as a function of eV/T, where V is the voltage and T is the boson temperature, based on Eqs. (24) and (25) in the equilibrium boson regime. Here, the parameter $a \equiv \alpha/\alpha_m$ is inversely proportional to the bosonic thermal mass $m_{\text{b}}^2 = \alpha_m T$ [see Eq. (6)]; $\bar{g}^2$ denotes the reduced squared Yukawa coupling. F_{adj} is suppressed as the interaction strength $\bar{g}^2$ increases (black to yellow). The parameters are $\gamma_{\text{el}} = 10$, $T = 0.05$, and $E_{\text{Th}} = 2 \times 10^{-3}$. Our plotted results for F_{adj} artificially approach $\sqrt{3}/4$ for $\bar{g}^2 = 0$ and $eV \gg T$ because of the assumed Fermi-Dirac distribution, Eq. (17). For $\bar{g}^2 > 0$, the device length L is always taken to be much longer than the electron-boson scattering length at the wire center. (c) and (d) indicate that the lack of well-defined quasiparticles gives a *weak enhancement* of the noise, on top of the main effect of dissipative suppression by the boson bath.

where c is a constant (see Fig. 2). Our results in Eqs. (3) and (4) are reminiscent of a holographic prediction [20]. The field appears through the combination $(eV)^2 E_{\text{Th}}$ in Eqs. (3) and

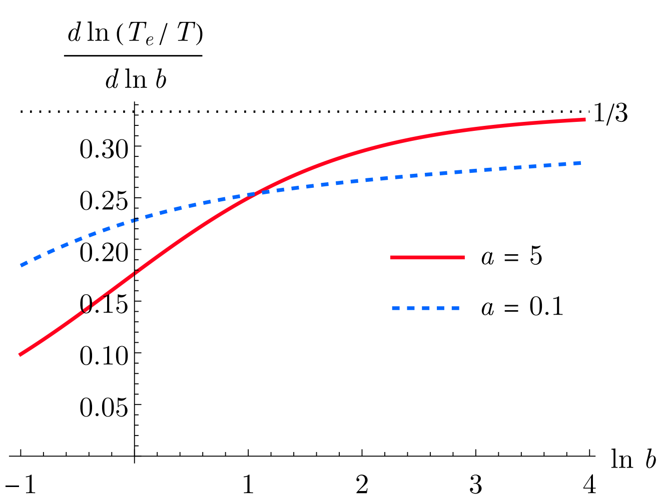

FIG. 2. Power-law dependence of T_e/T on $b \equiv (eV)^2 E_{\text{Th}}/(8T^3\bar{g}^2)$ for different a [see Eqs. (3) and (4)].

(4), relevant in the diffusive regime; here, $E_{\text{Th}} = D/L^2$ is the Thouless energy and L is the device length. The power law in Eq. (4) is consistent with the experimental data in Ref. [17], although we do not expect our 2D theory to apply directly to a bulk heavy-fermion material (see the Supplemental Material [21] for a more detailed analysis). The power in Eq. (3) differs from the electron-phonon result [14] because the latter depends upon the Debye energy; for the 2D MFL, only the dimensionless $\bar{g}^2$ enters.

When the bosons and leads reside at $T = 0$, we find

$$\mathsf{F}_{\text{adj}}(T = 0) = \mathsf{F} \simeq \frac{2T_{\text{eff}}}{eV} \mathcal{J}_0\left(\frac{\bar{g}^2 \pi\, T_{\text{eff}}}{\gamma_{\text{el}}}\right), \tag{5}$$

where $\mathcal{J}_0(y) = (1 + y)/(1 + y \ln 2)$ and the effective electronic temperature $T_{\text{eff}} = T_{\text{e}}(T = 0)$ in Eq. (3).

We focus here on the dirty MFL because recent theoretical studies suggest that disorder is crucial for strange metallicity observed in many quantum materials [18,22–24]. The interplay of disorder, Planckian dissipation, and quantum effects results in interesting consequences for transport [18,22–24] and superconductivity [19,25]. Due to disorder smearing, the critical bosonic propagator acquires a quantum relaxational form, with the retarded component being [18,23,24,26]

$$D^R_{\omega,\mathbf{q}} = -\left[2\left(q^2 - i\,\alpha\,\omega + m_{\text{b}}^2\right)\right]^{-1}. \tag{6}$$

Here, q is momentum, ω is frequency, $m_{\text{b}}^2 = \alpha_m T$ is the thermal mass arising due to quartic self-interactions among the bosons [18,23,24,27], while α and α_m are model-specific parameters. The quantum relaxational bosons give arise to a MFL self-energy [18,22–24,28] for electrons at equilibrium. The fermionic and bosonic propagators are in sharp contrast with their counterparts in the clean limit [29–31], and offer possible sources for the linear-T resistivity observed in strange metals [18,22–24].

We investigate the shot noise using the Keldysh formalism [1,32]. We evaluate the interaction corrections via the bubble [Fig. 3(a)] and Maki-Thompson diagrams (MT) [Fig. 3(b)] using the nonequilibrium electron distribution function. The latter is governed by the kinetic equation derived from the MFL-Finkel'stein nonlinear sigma model (MFL-FNLsM) [1,18]. For bosons staying in equilibrium, we will show that the excess noise is strongly suppressed by the dissipation. On the other hand, in the limit of strong electron-boson drag, contributions from the MFL self-energy and MT diagram cancel and we recover $\mathsf{F} = \sqrt{3}/4$ at $T = 0$ [13,14].

Model. We consider a 2D system with N flavors of spinless, disordered electrons at finite density coupled to SU(N) matrix quantum-critical bosons with a Yukawa coupling strength g [18,19,31,33] (formally in the unitary class [34,35]). We restrict our attention to onsite impurity potential disorder and ignore the Sachdev-Ye-Kitaev (SYK)-type randomness in g [36].

We focus on a wire geometry with a potential difference V applied across the sample along $\hat{x}$. We evaluate the shot noise in Eq. (1) by computing the the Keldysh component of the current-current correlator, which describes the correlation of the stochastic fluctuations of the electric current [1].

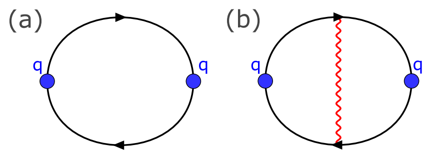

FIG. 3. Feynman diagrams for the Keldysh current-current correlation function: (a) the bubble diagram [Eq. (8)] and (b) the Maki-Thompson (MT) diagram [Eq. (10)]. Here, the black line is the fermion Green's function incorporating the MFL self-energy and disorder scattering, while the red wavy line represents the quantum relaxational bosonic propagator.

At the semiclassical level, we focus on the contribution due to the bubble [Fig. 3(a)] and MT diagrams [Fig. 3(b)]:

$$S_{\text{shot}} = S_{\text{B}} + S_{\text{MT}}. \tag{7}$$

The bold lines in the diagrams represent the fermionic Green's function at the saddle-point level [18], encoding the elastic scattering rate due to disorder and the MFL self-energy. We ignore the weak localization [1,37] and the Altshuler-Aronov quantum corrections [18,38] arising from the interplay between the diffusive collective modes and the quantum-critical bosons.

The shot noise due to the bubble diagram is

$$S_{\text{B}} = \sigma_{\text{D}} \int_0^L \frac{dx}{L} \int \frac{d\omega}{1 - \text{Im}\,\Sigma^R_\omega(x)/\gamma_{\text{el}}} \left[1 - F^2_\omega(x)\right], \tag{8}$$

where $\sigma_{\text{D}} = Ne^2\nu_0 D$ is the Drude conductivity, ν_0 is the density of states, L is the length of the wire, and the imaginary part of the nonequilibrium fermionic self-energy is [18]

$$\text{Im}\,\Sigma^R_\omega(x) = \frac{\bar{g}^2}{2}\int_{-\infty}^{\infty} d\nu \tan^{-1}\left(\frac{\alpha\nu}{m_{\text{b}}^2}\right)[F_{\omega+\nu}(x) - F_{B,\nu}(x)], \tag{9}$$

where $F_\varepsilon(x)$ and $F_{B,\varepsilon}(x)$ are respectively the generalized fermionic and bosonic distribution functions, which are governed by the kinetic equation discussed below. The center-of-mass position x dependence arises from the potential gradient applied across the wire. In the diffusive limit, the momentum dependence of the distribution functions is very weak and can be ignored. The corresponding equilibrium versions are $F^{\text{eq}}_\varepsilon = \tanh(\varepsilon/2T)$ and $F^{\text{eq}}_{B,\varepsilon} = \coth(\varepsilon/2T)$ [1,18,32,37]. In this case, Eq. (9) reduces to the MFL form [18].

On the other hand, the contribution from the MT diagram is [21]

$$S_{\text{MT}} = \frac{iNe^2}{2d}\int_0^L \frac{dx}{L} I_{\text{MT}}(x), \tag{10}$$

where $d = 2$ is the dimension, and

$$I_{\text{MT}}(x) \simeq 2i\,g^2\,v_F^2 \int_{\mathbf{k},\mathbf{q},\omega,\nu} 2\,\text{Im}\,D^R_{-\nu,-\mathbf{q}} \times G^R_{\omega,\mathbf{k}} G^A_{\omega,\mathbf{k}} G^R_{\omega+\nu,\mathbf{k}+\mathbf{q}} G^A_{\omega+\nu,\mathbf{k}+\mathbf{q}}\,\mathcal{F}(\omega,\nu), \tag{11}$$

the thermal factor

$$\mathcal{F}(\omega,\nu) = F_{B,-\nu}\left(F_\omega F_{\omega+\nu} - F^2_{\omega+\nu} + 1 - F^2_\omega\right) + F_\omega F_{\omega+\nu}(F_{\omega+\nu} - F_\omega), \tag{12}$$

and $G^{R/A}_{\omega,\mathbf{k}}$ is the retarded/advanced fermionic propagator. In the above expression, we have dropped terms that vanish by causality and ignored finite angle scattering terms. We explicitly check that S_{B} and S_{MT} reduce to the Johnson-Nyquist noise at equilibrium [21], as expected by the fluctuation-dissipation theorem [1,2].

It now remains to determine the distribution functions in order to compute the interaction corrections to the shot noise. The kinetic equation governing F_ω in the diffusive regime can be derived based on the saddle point of the MFL-FNLsM [1,18,21]. The result is

$$-D\,\nabla_x^2 F_\omega(x) = \mathfrak{St}_{\text{eb}}[F], \tag{13}$$

where $D = v_F^2/4\gamma_{\text{el}}$ is the diffusion constant and the electron-boson collision integral is given by

$$\mathfrak{St}_{\text{eb}}[F] = 4g^2 \int_{\Omega,\mathbf{q}} \text{Im}\,G^R_{\omega+\Omega,\mathbf{p}+\mathbf{q}}\,\text{Im}\,D^R_{\Omega,\mathbf{q}} \times \{F_{B,\Omega}(x)[F_{\omega+\Omega}(x) - F_\omega(x)] - [1 - F_{\omega+\Omega}(x)F_\omega(x)]\}. \tag{14}$$

In equilibrium, $\mathfrak{St}_{\text{eb}}[F] = 0$. $F_\omega(x)$ satisfies the boundary conditions

$$F_\omega(0) = \tanh\left(\frac{\omega}{2T}\right), \quad F_\omega(L) = \tanh\left(\frac{\omega - eV}{2T}\right). \tag{15}$$

Results. In the absence of interactions, $\mathfrak{St}_{\text{eb}}[F] = \text{Im}\,\Sigma^R_\omega(x) = 0$ and Eq. (13) has the standard solution

$$F^{\text{NI}}_\omega(x) = (1 - \bar{x})\tanh\left(\frac{\omega}{2T}\right) + \bar{x}\tanh\left(\frac{\omega - eV}{2T}\right), \tag{16}$$

where $\bar{x} = x/L$. Plugging Eq. (16) into Eq. (8) yields the Fano factor $\mathsf{F} = 1/3$.

With interactions, we focus on the kinetic regime $l_{\text{el}} \ll l_{\text{eb}} \ll L$, where l_{el} (l_{eb}) is the elastic (inelastic) scattering length due to impurities (electron-boson collisions). In this "hydrodynamic" limit, both the fermion and boson distribution functions are expected to reflect local equilibration throughout the bulk of the wire, although deviations can occur near the contacts. Even with this constraint, however, different limits are possible, depending upon the relationship between the local electron and boson temperatures.

If electron-boson collisions occur much more frequently than boson-boson scattering, then the bosons are driven away from equilibrium with the electrons and share a common local temperature (electron-boson drag regime). The distribution function F_ω acquires a local Fermi-Dirac form,

$$F^{\text{hydro}}_\omega(x) = \tanh\left[\frac{\omega - eV\,\bar{x}}{2T_{\text{e}}(\bar{x})}\right], \tag{17}$$

and $F_{B,\Omega}$ acquires a local Bose form,

$$F^{\text{hydro}}_{B,\omega}(x) = \coth\left[\frac{\omega}{2T_{\text{e}}(\bar{x})}\right], \tag{18}$$

nullifying the collision integral in Eq. (14). The local temperature profile $T_{\text{e}}(\bar{x})$ can be determined using Eq. (13) subjected to the boundary conditions $T_{\text{e}}(0) = T_{\text{e}}(1) = T$ [14]. In this limit, the self-energy term $\Sigma^R_\omega(x)$ in S_{B} [Eq. (8)] is canceled

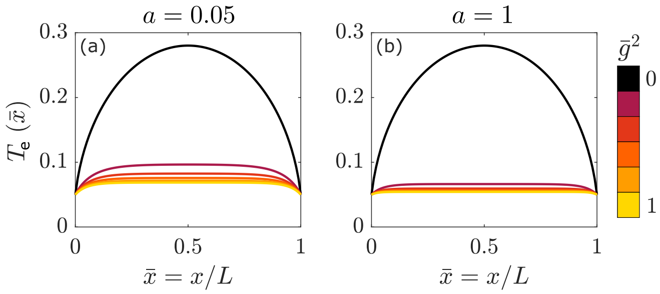

FIG. 4. Plot of the electron temperature profile $T_e(\bar{x})$ obtained by solving Eq. (19). As the interaction coupling strength $\bar{g}^2$ increases, T_e decreases, which suppresses the shot noise as a result. With a larger bosonic thermal mass (smaller a), the suppression to T_e is weakened due to thermal screening. In the long wire limit with a finite $\bar{g}^2$, T_e is essentially a constant except in proximity to the contacts. Here, $\gamma_{el} = 10$, $T = 0.05$, $E_{Th} = 2 \times 10^{-3}$, and $V = 1$.

by S_{MT} [Eq. (10)] [21], as also occurs in the dc conductivity calculation [18,23,24]. As a result, $\mathsf{F} = \sqrt{3}/4$ for $T \to 0$ [14].

The physics is more interesting if we assume that the fermions acquire a hydrodynamic distribution function [Eq. (17)] while the bosons remain at equilibrium, i.e., $F_{B,\omega} = F^{eq}_{B,\omega}$, which can happen due to the boson-boson self-interactions, boson-impurity collisions, and other sources of scattering. In this regime, we can integrate both sides of Eq. (13) to obtain a diffusion equation for the electron temperature profile T_e [14],

$$\frac{\pi^2}{6}\nabla^2_{\bar{x}} T_e^2(\bar{x}) = -(eV)^2 + \frac{1}{2E_{Th}}\int_{-\infty}^{\infty} d\omega\, \omega\, \mathfrak{St}_{eb}[F], \quad (19)$$

where $E_{Th} = D/L^2$ is the Thouless energy. We numerically solve for T_e using Eq. (19) and the results are shown in Fig. 4. In the long-wire limit ($L \to \infty$), the Laplacian term in Eq. (19) can be dismissed and T_e remains constant except in proximity to the contacts. At low T, T_e can be solved approximately to give Eq. (3) [21], which is consistent with the numerics.

Evaluating the shot noise using Eqs. (7), (8), (10), and (17), we have

$$S_{shot} = 4\,\sigma_D \int_0^1 d\bar{x}\, T_e(\bar{x})\, \mathcal{J}(\bar{x}, \bar{g}^2, T), \quad (20)$$

where

$$\mathcal{J}(\bar{x}, \bar{g}^2, T) = \frac{1}{2}\int_{-\infty}^{\infty} d\bar{\omega}\, \frac{\mathcal{I}_B(\bar{x}, \bar{\omega}) + \mathcal{I}_{MT}(\bar{x}, \bar{\omega})}{1 - \operatorname{Im}\Sigma^R_{2T_e\bar{\omega}}(\bar{x})/\gamma_{el}}, \quad (21)$$

$$\mathcal{I}_B(\bar{x}, \bar{\omega}) = 1 - \tanh^2(\bar{\omega} - eV\,\bar{x}/2T_e), \quad (22)$$

and

$$\mathcal{I}_{MT}(\bar{x}, \bar{\omega}) = -\frac{\bar{g}^2 T_e}{\gamma_{el}}\int_{-\infty}^{\infty} d\bar{\nu}\, \tan^{-1}\left(\frac{2a\,T_e\bar{\nu}}{T}\right)\mathcal{F}(2T_e\bar{\omega}, 2T_e\bar{\nu}). \quad (23)$$

Here, the parameter $a = \alpha/\alpha_m$ and the position dependence on T_e is implicit. The corresponding formal Fano factor (defined here for general eV/T) is

$$\mathsf{F} = \frac{2}{eV}\int_0^1 d\bar{x}\, T_e(\bar{x})\mathcal{J}(\bar{x}, \bar{g}^2, T). \quad (24)$$

In the integrand, $T_e(\bar{x})$ arises from the solution to the kinetic equation, as occurs for electron-phonon scattering [16], while $\mathcal{J}(\bar{x}, \bar{g}^2, T)$ [Eq. (21)] encodes MFL corrections that slightly enhance F. Despite its complicated form, S_{shot} can be evaluated analytically at $T = 0$, resulting in Eq. (5) [21]. Numerical results for $T > 0$ are shown in Figs. 1(a) and 1(b).

We quantify the effects of the MFL self-energy and the Maki-Thompson (MT) diagram through the ratio

$$\mathcal{R}(\bar{g}, T) = \int_0^1 d\bar{x}\, T_e(\bar{x})\mathcal{J}(\bar{x}, T, \bar{g}^2)\left[\int_0^1 d\bar{x}\, T_e(\bar{x})\right]^{-1}, \quad (25)$$

which is illustrated in Figs. 1(c) and 1(d). Since the bosons and fermions do not share the same temperature, i.e., $T \neq T_e(0 < \bar{x} < 1)$, the contribution from $\Sigma^R_\omega(x)$ is not canceled, in contrast with the boson-fermion drag and linear response regimes. Similar to the phonon suppression mechanism, F_{adj} decreases as the wire length L and the coupling strength $\bar{g}^2$ increase. The MFL effects encoded in $\mathcal{J}$ and $\mathcal{R}(\bar{g}, T)$ produce a weak enhancement to the noise.

Conclusion. We have developed a theory for the suppression of shot noise in a 2D disordered MFL at the semiclassical level using the Keldysh framework. Our theory reproduces known results in the noninteracting and electron-boson drag limits. If the quantum-relaxational bosons remain in equilibrium, shot noise is strongly suppressed in the nonuniversal manner described by Eq. (24). This scenario may be relevant to the recent experiment [17,21].

Our theory features a power-law temperature dependence in the shot noise [Eqs. (3) and (4)], with an exponent that can differentiate noise suppression mechanisms due to quantum-critical bosons versus phonons [14,16]. Our results imply that the suppression of shot noise does not necessarily correlate to the absence of quasiparticles [17]. In fact, we find that the nonequilibrium MFL self-energy and vertex correction instead *weakly boost* the shot noise on top of the dissipative suppression due to the bosons [Figs. 1(c) and 1(d)].

Our results contrast with a recent theory proposed in Ref. [42], where a universal Fano factor of 1/6 is obtained in the large-interaction variance limit $g'^2 \to \infty$ using the SYK-type model with spatially random Yukawa couplings at $T = 0$. The differences arise from the form of the electron distribution function used; both calculations consider bosons in equilibrium. We focus on the kinetic regime where $l_{el} \ll l_{eb} \ll L$, which generically admits electron and boson distribution functions of local equilibrium form [16]. Moreover, for a fixed voltage V, the Fano factor in Ref. [42] is independent of L whereas our result vanishes as $L \to \infty$ (for either fixed voltage V or electric field strength V/L). Physically, as the length of the nanowire increases, we expect the shot noise to be further suppressed due to additional dissipation, consistent with the case of electron-phonon interactions [16].

There are numerous intriguing avenues that merit further investigations. From a theoretical perspective, it would be interesting to explore the weak localization [1,37] and Altshuler-Aronov [18,38] quantum corrections to shot noise. It would also be valuable to explore the effects of other impurity distributions and the consequences a nonequilibrium bosonic temperature by solving a separate kinetic equation for the bosons. On the experimental front, it would be captivating to measure the shot noise in other quantum-critical systems to determine the universality of the results and to test the predicted power-law temperature dependence. On the other hand, it is worthwhile to explore the local temperature profile of the nanowire, which can offer valuable insights into unveiling the physical distribution function.

Acknowledgments. We thank Maxim Dzero, Alex Kamenev, Alex Levchenko, Doug Natelson, and Yiming Wang for useful discussions. We are grateful to Doug Natelson and Liyang Chen for sending us the experimental data. This work was supported by the Welch Foundation Grant No. C-1809 (T.C.W. and M.S.F.).

[1] A. Kamenev, *Field Theory of Non-Equilibrium Systems*, 2nd ed. (Cambridge University Press, Cambridge, UK, 2023).
[2] Ya. M. Blanter and M. Büttiker, Shot noise in mesoscopic conductors, Phys. Rep. **336**, 1 (2000).
[3] P. Zhou, L. Chen, Y. Liu, I. Sochnikov, A. T. Bollinger, M.-G. Han, Y. Zhu, X. He, I. Bozovic, and D. Natelson, Electron pairing in the pseudogap state revealed by shot noise in copper oxide junctions, Nature (London) **572**, 493 (2019).
[4] R. de-Picciotto, M. Reznikov, M. Heiblum, V. Umansky, G. Bunin, and D. Mahalu, Direct observation of a fractional charge, Nature (London) **389**, 162 (1997).
[5] L. Saminadayar, D. C. Glatti, Y. Jin, and B. Etienne, Observation of the $e/3$ fractionally charged Laughlin quasiparticle, Phys. Rev. Lett. **79**, 2526 (1997).
[6] T. Delattre, C. Feuillet-Palma, L. G. Herrmann, P. Morfin, J.-M. Berroir, G. Fève, B. Plaçais, D. C. Glattli, M.-S. Choi, C. Mora, and T. Kontos, Noisy Kondo impurities, Nat. Phys. **5**, 208 (2009).
[7] O. Zarchin, M. Zaffalon, M. Heiblum, D. Mahalu, and V. Umansky, Two-electron bunching in transport through a quantum dot induced by Kondo correlations, Phys. Rev. B **77**, 241303(R) (2008).
[8] Sh. M. Kogan and A. Ya. Shul'man, Theory of fluctuations in a nonequilibrium electron gas, Zh. Eksp. Teor. Fiz. **56**, 862 (1969) [Sov. Phys. JETP **29**, 467 (1969)].
[9] C. W. J. Beenakker and M. Büttiker, Suppression of shot noise in metallic diffusive conductors, Phys. Rev. B **46**, 1889 (1992).
[10] K. E. Nagaev, On the shot noise in dirty metal contacts, Phys. Lett. A **169**, 103 (1992).
[11] B. L. Altshuler, L. S. Levitov, and A. Y. Yakovets, Nonequilibrium noise in a mesoscopic conductor: A microscopic analysis, JETP Lett. **59**, 857 (1994).
[12] Y. V. Nazarov, Limits of universality in disordered conductors, Phys. Rev. Lett. **73**, 134 (1994).
[13] V. I. Kozub and A. M. Rudin, Shot noise in mesoscopic diffusive conductors in the limit of strong electron-electron scattering, Phys. Rev. B **52**, 7853 (1995).
[14] K. E. Nagaev, Influence of electron-electron scattering on shot noise in diffusive contacts, Phys. Rev. B **52**, 4740 (1995).
[15] Y. Wang, C. Setty, S. Sur, L. Chen, S. Paschen, D. Natelson, and Q. Si, Shot noise as a characterization of strongly correlated metals, arXiv:2211.11735.
[16] A. Levchenko and J. Schmalian, Transport properties of strongly coupled electron-phonon liquids, Ann. Phys. **419**, 168218 (2020).
[17] L. Chen, D. T. Lowder, E. Bakali, A. M. Andrews, W. Schrenk, M. Waas, R. Svagera, G. Eguchi, L. Prochaska, Y. Wang, C. Setty, S. Sur, Q. Si, S. Paschen, and D. Natelson, Shot noise indicates the lack of quasiparticles in a strange metal, Science **382**, 907 (2023).
[18] T. C. Wu, Y. Liao, and M. S. Foster, Quantum interference of hydrodynamic modes in a dirty marginal Fermi liquid, Phys. Rev. B **106**, 155108 (2022).
[19] T. C. Wu, P. A. Lee, and M. S. Foster, Enhancement of superconductivity in a dirty marginal Fermi liquid, Phys. Rev. B **108**, 214506 (2023).
[20] J. Sonner and A. G. Green, Hawking radiation and nonequilibrium quantum critical current noise, Phys. Rev. Lett. **109**, 091601 (2012).
[21] See Supplemental Material at http://link.aps.org/supplemental/10.1103/PhysRevB.110.L081102 for the Keldysh computation of the diagrams, the derivation and solution to the kinetic equation, the derivation of Eq. (5), and the comparison of experimental data from Ref. [17] to Eq. (4), which includes Refs. [39–41].
[22] I. Esterlis, H. Guo, A. A. Patel, and S. Sachdev, Large-N theory of critical Fermi surfaces, Phys. Rev. B **103**, 235129 (2021).
[23] H. Guo, A. A. Patel, I. Esterlis, and S. Sachdev, Large-N theory of critical Fermi surfaces II: Conductivity, Phys. Rev. B **106**, 115151 (2022).
[24] A. A. Patel, H. Guo, I. Esterlis, and S. Sachdev, Universal theory of strange metals from spatially random interactions, Science **381**, 790 (2023).
[25] P. A. Nosov, I. S. Burmistrov, and S. Raghu, Interplay of superconductivity and localization near a 2D ferromagnetic quantum critical point, Phys. Rev. B **107**, 144508 (2023).
[26] V. M. Galitski, Metallic phase in a two-dimensional disordered Fermi system with singular interactions, Phys. Rev. B **72**, 214201 (2005).
[27] J. A. Damia, M. Solís, and G. Torroba, How non-Fermi liquids cure their infrared divergences, Phys. Rev. B **102**, 045147 (2020).
[28] C. M. Varma, P. B. Littlewood, S. Schmitt-Rink, E. Abrahams, and A. E. Ruckenstein, Phenomenology of the normal state of Cu-O high-temperature superconductors, Phys. Rev. Lett. **63**, 1996 (1989).
[29] S.-S. Lee, Recent developments in non-Fermi liquid theory, Annu. Rev. Condens. Matter Phys. **9**, 227 (2018).
[30] S. Sachdev, *Quantum Phase Transitions*, 2nd ed. (Cambridge University Press, Cambridge, UK, 2011).
[31] J. A. Damia, S. Kachru, S. Raghu, and G. Torroba, Two-dimensional non-Fermi-liquid metals: A solvable large-N limit, Phys. Rev. Lett. **123**, 096402 (2019).
[32] A. Kamenev and A. Levchenko, Keldysh technique and nonlinear σ-model: basic principles and applications, Adv. Phys. **58**, 197 (2009).
[33] P. A. Nosov, I. S. Burmistrov, and S. Raghu, Interaction-

induced metallicity in a two-dimensional disordered non-Fermi liquid, Phys. Rev. Lett. **125**, 256604 (2020).

[34] A. Altland and M. R. Zirnbauer, Nonstandard symmetry classes in mesoscopic normal-superconducting hybrid structures, Phys. Rev. B **55**, 1142 (1997).

[35] S. Ryu, A. P. Schnyder, A. Furusaki, and A. W. W. Ludwig, Topological insulators and superconductors: tenfold way and dimensional hierarchy, New J. Phys. **12**, 065010 (2010).

[36] D. Chowdhury, A. Georges, O. Parcollet, and S. Sachdev, Sachdev-Ye-Kitaev models and beyond: Window into non-Fermi liquids, Rev. Mod. Phys. **94**, 035004 (2022).

[37] Y. Liao, A. Levchenko, and M. S. Foster, Response theory of the ergodic many-body delocalized phase: Keldysh Finkel'stein sigma models and the 10-fold way, Ann. Phys. **386**, 97 (2017).

[38] D. B. Gutman and Y. Gefen, Shot noise in disordered junctions: Interaction corrections, Phys. Rev. B **64**, 205317 (2001).

[39] T. C. Wu, H. K. Pal, and M. S. Foster, Topological anomalous skin effect in Weyl superconductors, Phys. Rev. B **103**, 104517 (2021).

[40] D. L. Maslov and A. V. Chubukov, First-Matsubara-frequency rule in a Fermi liquid. II. Optical conductivity and comparison to experiment, Phys. Rev. B **86**, 155137 (2012).

[41] A. M. Finkel'stein, Influence of Coulomb interaction on the properties of disordered metals, Zh. Eksp. Teor. Fiz. **84**, 168 (1983) [Sov. Phys. JETP **57**, 97 (1983)].

[42] A. Nikolaenko, S. Sachdev, and A. A. Patel, Theory of shot noise in strange metals, Phys. Rev. Res. **5**, 043143 (2023).